

Scenario of strongly non-equilibrium Bose-Einstein condensation

Natalia G. Berloff¹ and Boris V. Svistunov²

¹*Department of Mathematics, University of California, Los Angeles, CA, USA, 90095-1555*

²*Russian Research Center “Kurchatov Institute”, 123182 Moscow, Russia
nberloff@math.ucla.edu, svist@kurm.polym.kiae.su*

(February 7, 2020)

Large scale numerical simulations of the Gross-Pitaevskii equation are used to elucidate the self-evolution of a Bose gas from a strongly non-equilibrium initial state. The stages of the process confirm and refine the theoretical scenario of Bose-Einstein condensation developed by Svistunov, Kagan, and Shlyapnikov [1–3]: the system evolves from the regime of weak turbulence to superfluid turbulence, via states of strong turbulence in the long-wavelength region of energy space.

The experimental realization of Bose-Einstein condensates (BEC) in dilute alkali and hydrogen gases [4] and more recently in a gas of metastable helium [5] has stimulated a great interest in the dynamics of BEC. In the case of a pure condensate, both equilibrium and dynamical properties of the system can be described by the Gross-Pitaevskii (GP) equation [6]. The GP model has been remarkably successful in predicting the condensate shape in an external potential, the dynamics of the expanding condensate cloud, the motion of quantized vortices; it is also a popular qualitative model of superfluid helium.

The important and often overlooked feature of the GP model is that it gives an accurate microscopic description of the formation of BEC from the (strongly degenerate) gas of weakly interacting bosons [7,8]. By large scale numerical simulations of the GP equation it is possible, in principle, to reveal all the stages of this evolution from weak turbulence to superfluid turbulence with a tangle of quantized vortices, as was argued by Svistunov, Kagan, and Shlyapnikov [1–3] (for a brief review see [9]). This task has up to now remained unfulfilled, though some important steps in this direction have been made [10,11]. The goal of this Letter is to carry out this task. We are mainly interested in tracing the development, at a certain stage of evolution, of the so-called coherent regime [7,1–3]. The onset of this regime corresponds to the breakdown of the regime of weak turbulence in a low-energy region of wavenumber space and leads to the formation of superfluid short-range order (the state of superfluid turbulence, characterized by quasi-condensate local correlation properties [1–3]). The transition from weak turbulence to superfluid turbulence is a key ordering process in macroscopically large systems. A rigorous theoretical (and also a numerical or experimental) study of this stage of evolution has been lacking. The general conclusions concerning this stage [2,3] were made on the basis of qualitative analysis, which naturally contained *ad hoc* elements.

The classical-field description of the strongly degen-

erate weakly interacting Bose gas is given by the GP equation as

$$i\hbar \frac{\partial \psi}{\partial t} = -\frac{\hbar^2}{2m} \nabla^2 \psi + U |\psi|^2 \psi, \quad (1)$$

where ψ is the complex-valued classical field, $|\psi|^2$ being equal to the particle number density, m is the mass of the boson, $U = 4\pi\hbar^2 a/m$ is the strength of the δ -function interaction (pseudo-)potential, and a is the scattering length. It is important to emphasize that the only essential restriction on the applicability of this model is that the occupation numbers are much larger than unity (see, e.g., [8]). In the context of the problem of BEC kinetics, this requirement is automatically satisfied: the evolution leads to an explosive increase of occupation numbers in the low-energy region of wavenumber space [1], where the ordering process takes place. This means that the requirement of large occupation numbers is not a restrictive one. Even when the evolution starts with occupation numbers of order unity, so that the classical-field description is not yet applicable, the evolution (which can be described at this stage by the standard Boltzmann quantum kinetic equation) inevitably leads to the appearance of large occupation numbers in the low-energy tail of the particle distribution (see, e.g., [12]). Since the ordering kinetics obeys the blow-up scenario [1–3] and only the low-energy part of the field is initially involved in the process, one can safely switch from the kinetic equation to the classical-field description (for the long-wavelength component of the field) at a certain moment in the evolution, when the occupation numbers become large enough.

In what follows we consider the evolution of (1) starting with a strongly non-equilibrium initial condition $\psi(\mathbf{r}, t = 0) = \sum_{\mathbf{k}} a_{\mathbf{k}} \exp(i\mathbf{k}\mathbf{r})$, where the phases of the complex amplitudes $a_{\mathbf{k}}$ are distributed randomly. Such an initial condition follows from the microscopic quantum-mechanical analysis of the state of a weakly interacting Bose gas in the kinetic regime [8]. Theoretical investigations of the relaxation of such an initial state towards the equilibrium configuration were performed by Svistunov, Kagan, and Shlyapnikov [1–3]. The analy-

sis revealed a number of stages in the evolution. Initially the system is in the weak turbulence regime and thus can be described by the Boltzmann kinetic equation. Such an equation is obtained as the random-phase approximation of (1) for occupation numbers $n_{\mathbf{k}}$ defined by $\langle a_{\mathbf{k}} a_{\mathbf{k}'}^* \rangle \approx n_{\mathbf{k}} \delta_{\mathbf{k}} \delta_{\mathbf{k}'}$. Alternatively, the weak-turbulence kinetic equation follows from the general quantum Boltzmann kinetic equation, if one neglects spontaneous scattering as compared with stimulated scattering (because of the large occupation numbers). Svistunov [1], and later Semikoz and Tkachev [12], considered the self-similar solution of the Boltzmann kinetic equation:

$$n_{\epsilon}(t) = A \epsilon_0^{-\alpha}(t) f(\epsilon/\epsilon_0), \quad t \leq t^*, \quad (2)$$

$$\epsilon_0(t) = B(t^* - t)^{1/2(\alpha-1)}, \quad (3)$$

$$f(x) \rightarrow x^{-\alpha} \quad \text{at } x \rightarrow \infty, \quad f(0) = 1, \quad (4)$$

where $\epsilon = \hbar^2 k^2 / 2m$. The dimensional constants A and B relate to each other by $(\alpha - 1)m^3 U^2 A^2 = \lambda \pi^3 \hbar^7 B^{2(\alpha-1)}$, where the parameters α and λ were determined by numerical analysis as $\alpha \approx 1.24$ [12] and $\lambda \approx 1.2$ [1]. The form of the function f was also determined numerically [1]. The solution (2)-(4) has only one free parameter, say A , that depends on conditions in the ‘‘pre-historic’’ evolution.

The self-similar solution (2)-(4) corresponds to a wave in the energy space, propagating from high to lower energies. The energy $\epsilon_0(t)$ defines the ‘‘head’’ of the wave. The wave propagates in a blow-up fashion: $\epsilon_0(t) \rightarrow 0$ and $n_{\epsilon_0}(t) \rightarrow \infty$ as $t \rightarrow t^*$. In reality, the validity of the kinetic equations, associated with the random phase approximation, breaks down shortly before the blow-up time t^* . This moment marks the beginning of a qualitatively different stage in the evolution (the coherent regime): the strong turbulence evolves into a quasi-condensate state. In the coherent regime the phases of the complex amplitudes $a_{\mathbf{k}}$ of the field ψ become strongly correlated and the periods of their oscillations are then comparable with the evolution times of the occupation numbers. The formation of the quasi-condensate is manifested by the appearance of a well-defined tangle of quantized vortices and by the beginning of the final stage of the evolution: superfluid turbulence. In this regime the vortex tangle starts to relax over macroscopically large times.

To observe these stages of evolution we performed a large scale numerical integration of the GP equation (1) starting with strongly non-equilibrium initial condition. Our calculations were done in a periodic box N^3 , with $N = 256$, using a fourth-order (with respect to the spatial variables) finite-difference scheme. The scheme corresponds to the Hamiltonian system in the discrete variables ψ_{ijk} :

$$i \frac{\partial \psi_{ijk}}{\partial t} = \frac{\partial H}{\partial \psi_{ijk}^*}, \quad (5)$$

where $H = \frac{1}{2} \sum_{ijk} \psi_{ijk}^* \left[-\frac{1}{12} (\psi_{i+2,j,k} - \psi_{i-2,j,k} + \psi_{i,j+2,k} - \psi_{i,j-2,k} + \psi_{i,j,k+2} - \psi_{i,j,k-2}) + \frac{4}{3} (\psi_{i+1,j,k} - \psi_{i-1,j,k} + \psi_{i,j+1,k} - \psi_{i,j-1,k} + \psi_{i,j,k+1} - \psi_{i,j,k-1}) \right] - \frac{1}{2} |\psi_{ijk}|^4$ [in the numerics we used the units $\hbar = m = 1$, $U = 1/2$, and set the space step in each direction of the grid as $dx = dy = dz = 1$]. Equation (5) conserves the energy H and the total particle number $\sum_{ijk} |\psi_{ijk}|^2$ exactly. In time stepping the leap-frog scheme was implemented with a backward Euler step every 10,000 steps to prevent the even-odd instability. The leap-frog scheme is nondissipative, so the only loss of energy and of the total particle number occurs during the backward Euler step and, since we take this step very rarely, these losses are insignificant. The code was tested against known solutions of the GP model: vortex rings and rarefaction pulses [13]. The calculations were performed on a Sun Enterprise 450 Server and took about three months to complete for the main set of calculations discussed below.

To eliminate the computationally expensive (and the least physically interesting) transient regime, we started directly from the self-similar solution (2)-(4):

$$a_{\mathbf{k}} = \sqrt{\xi_{\mathbf{k}} n_0 f(\epsilon/\epsilon_0)} \exp[i\phi_{\mathbf{k}}], \quad (6)$$

where $\xi_{\mathbf{k}}$ and $\phi_{\mathbf{k}}$ are random numbers. [Note that in the simulations the momentum \mathbf{k} is the momentum of the lattice Fourier transform.] The phase $\phi_{\mathbf{k}}$ is uniformly distributed on $[0, 2\pi]$, in accordance with the basic statement of the theory of weak turbulence and, with the explicit microscopic analysis of corresponding quantum field states [8]. The choice of $\xi_{\mathbf{k}}$ is rather arbitrary (we only fix its mean value to be equal to unity, introducing therefore the parameter n_0) [14].

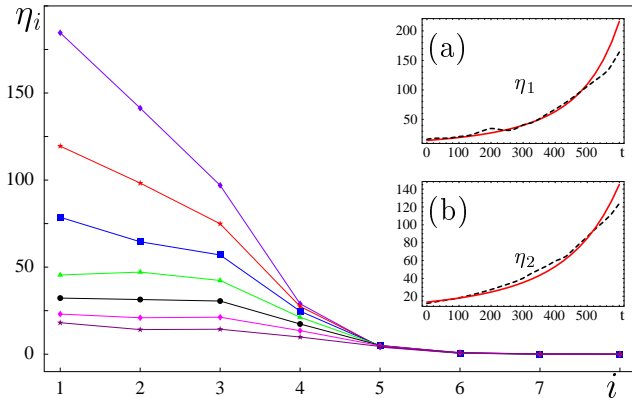
When choosing the parameters of the initial condition specified by the complex Fourier amplitudes (6), we have to take ϵ_0 small enough, to be free from systematic error of large finite-differences. On the other hand, taking ϵ_0 too small reduces the physical size of the system. Let us define one period of the amplitude oscillation as $t_p = 2\pi/\epsilon_0$ and the number of periods before the blow-up as $P = t^*/t_p$. When choosing the value of n_0 , in combination with ϵ_0 , we would like to avoid having P too small, when the time scale of the kinetic regime becomes too short, or having P too large, when the finite-size effects (the discreteness of the \mathbf{k}) dominate the calculation. Given the maximal available grid size $N = 256$, we found that it is optimal to take $n_0 = 15$ and $\epsilon_0 = 1/18$, so that $t_p \approx 113$, $t^* = 4\lambda\pi^3/(\alpha - 1)\epsilon_0^2 n_0^2 \approx 893$, and $P \approx 8$.

The instantaneous values of the occupation numbers $n_{\mathbf{k}}(t) = |a_{\mathbf{k}}(t)|^2$ are extremely ‘noisy’ functions of time. To be able to draw some quantitative comparisons and conclusions we need either to perform some averaging or to deal with some coarse-grained self-averaging characteristics of the particle distribution. Taking the second option, we introduce *shells* in momentum space. By the

i -th shell ($i = 1, 2, 3, \dots$) we understand the set of momenta, satisfying the condition $i - 1 \leq \log_2(k/2\pi) < i$. Each shell represents some characteristic scale of momentum (wavelength), and it is reasonable to define the average over the shell i of the occupation number: $\eta_i(t) = \sum^{(\text{shell } i)} n_{\mathbf{k}}(t)/M_i$, where M_i is the number of harmonics in the i -th shell. The harmonic $\mathbf{k} = 0$, which plays a special role (at the very end of the evolution), is not assigned to any shell. We also found it is rather instructive to keep track of the evolution of the integral distribution function $F_k = \sum_{k' \leq k} n_{k'}$.

The self-similar character of the evolution is clearly observed in Fig. 1. Inserts in Fig. 1 give the comparison of the theoretical prediction of the evolution of the occupation number function $n_\epsilon(t)$ defined by (2) and the evolution of the first and the second shells. The agreement with the theoretical predictions [1] is quite good for $t < 600$. After that the numerical solution deviates from the self-similar theoretical solution, which is the manifestation of the onset of the strong turbulence stage of evolution.

FIG. 1. The time evolution of $\eta_i(t = 100j)$ in the weak turbulence regime for $j = 0, \dots, 6$. In the insets we show the theoretical self-similar solution (2)-(4) (solid line) and the solution obtained through the numerical integration of (1) (dashed line) for the shells $i = 1$ (a) and $i = 2$ (b).



As follows from dimensional analysis (see, e.g., [9]), the characteristic time, t_0 , and the characteristic wave vector, k_0 , at the beginning of the strong turbulence regime are given by the relations

$$t_* - t_0 \sim C_0 [\hbar^{2\alpha+5}/m^3 U^2 A^2]^{1/(2\alpha-1)}, \quad (7)$$

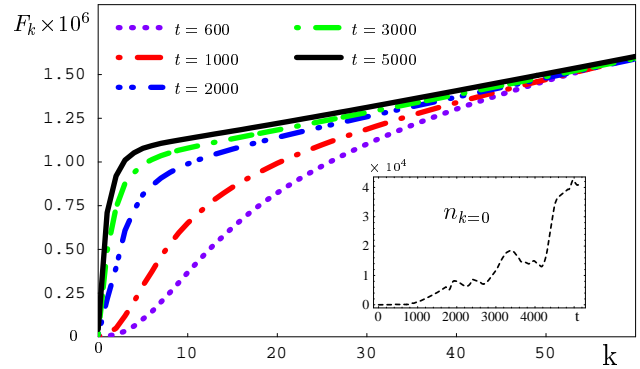
$$k_0 \sim C_1 [AU(m/\hbar)^{\alpha+1}]^{1/(2\alpha-1)}, \quad (8)$$

where C_0 are C_1 some dimensionless constants. Our numerical results (Fig. 1) indicate that $t_* - t_0 \sim 300$, which implies $C_0 \sim 40$.

After the formation of the quasi-condensate ($t > 1000$), the distribution of particles acquires a bimodal shape, which is clearly seen in Fig. 2. The salient characteristic of the distribution is the shoulder, which becomes

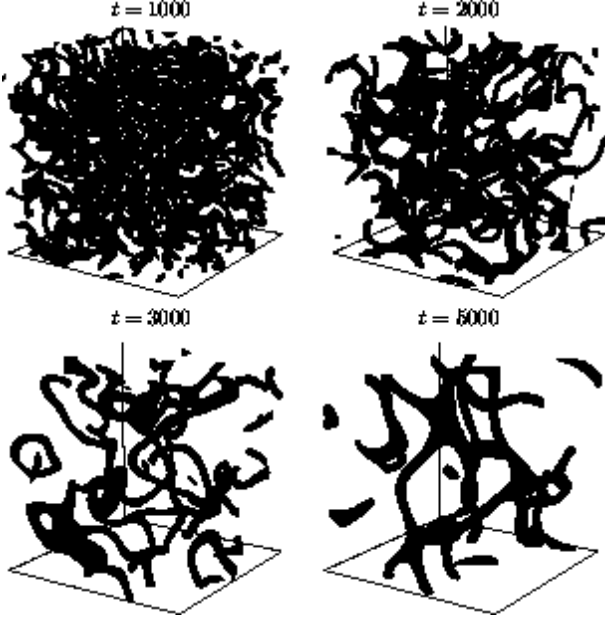
sharper and sharper as the evolution continues. Note that, by definition of the function F_k , the height of the shoulder is equal to the number of the quasi-condensate particles. From Fig. 2 we estimate $k_0 \sim 15$, which means that $C_1 \sim C_0 \sim 40$.

FIG. 2. Evolution of the integral distribution of particles $F_k = \sum_{k' \leq k} n_{k'}$. Notice the appearance of a ‘shoulder’ of F_k as the quasi-condensate is being formed. The evolution of $n_{k=0}$ is presented in the inset. Note the strong fluctuations, typical for the evolution of a single harmonic. The fluctuations are also noticeable in the graph of the first shell (see insert (a) of Fig. 1).



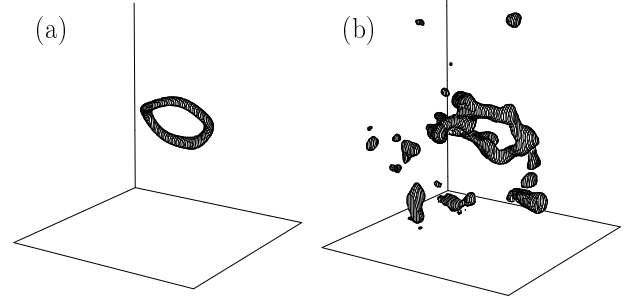
Within the coherent regime, the momentum distribution of the harmonics yields rather incomplete picture of the evolution, and it becomes reasonable to follow the ordering process in coordinate space. The most important is tracing the topological defects in the phase of the long-wavelength part of the complex field ψ , since the transformation of these defects into a tangle of well-separated vortex lines is the most essential feature of the superfluid short-range ordering [3]. To this end we first filter out the high-frequency harmonics by performing the transformation $a_{\mathbf{k}} \rightarrow a_{\mathbf{k}} \max\{1 - k^2/k_c^2, 0\}$, where k_c is a cut-off wave number. When the quasi-condensate has a pronounced shoulder the natural choice is to take k_c somewhat larger than k for the shoulder in order to remove the above-the-condensate part of the field ψ [15]. The results of visualizing the topological defects are presented in Fig. 3. The formation of a tangle of well-separated vortices (the state of superfluid turbulence) and the decay of superfluid turbulence are clearly seen. Notice that the characteristic time of the evolution depends on the average interline spacing, R , as $R^2/\ln(R/a_0)$, where a_0 is the vortex core size [3]. During the final stage of this evolution R is of order of a linear dimension of the computational box. To observe this final stage of the decay of superfluid turbulence we repeated the calculations for a smaller computational box with $N = 128$ (reducing in this way the computational time by a factor of $\sim 32 = 2^3 \times 2^2$). A single vortex ring remains at $t = 4000$ as the result of the turbulence decay; see Fig. 4(a).

FIG. 3. Evolution of topological defects in the phase of the long-wavelength part $\tilde{\psi}$ of the field ψ . The defects are visualized by isosurfaces $|\tilde{\psi}|^2 = 0.05\langle|\tilde{\psi}|^2\rangle$. High-frequency spatial waves are suppressed by the factor $\max\{1 - k^2/k_c^2, 0\}$, where the cut-off wave number is chosen according to the phenomenological formula $k_c = 9 - t/1000$.



The filtering method mentioned above allows us to visualize the positions of the core of the quantized vortex lines, but not the actual size of the core, since we force the solution to be represented by a relatively small number of harmonics. To get a better representation of an actual size of the core as well as of some other objects of interest such as rarefaction pulses, we implemented a different type of filtering, through a time averaging process. Fig. 4 compares the isosurfaces of the particle density obtained by two different methods: by high-frequency suppression (Fig. 4a) and by time averaging (Fig. 4b).

FIG. 4. Comparison of two isosurfaces obtained by different filtering techniques. The solution at $t = 4000$ is obtained by numerical integration of (1) in the periodic box with $N = 128$. Parameters of the initial condition are $\epsilon = 1/2$ and $n_0 = 2\pi$, so that the number of periods before the blow-up (see the text) is $P \approx 5$. The isosurface $|\tilde{\psi}|^2 = 0.05\langle|\tilde{\psi}|^2\rangle$ is plotted in Fig. 4(a) using the high-frequency filtering with $k_c = 5$. The isosurface $|\hat{\psi}|^2 = 0.2\langle|\hat{\psi}|^2\rangle$ is plotted in Fig. 4(b), where $\hat{\psi}_{ijk}(t) = \int \psi_{ijk}(\tau) \exp[-(\tau - t)^2/100] d\tau$.



In summary, we outline the most important features of the scenario observed. The low-energy part of the quantum field, characterized by large occupation numbers, and thus described by a classical complex field ψ obeying Eq. (1), initially evolves in a weak-turbulent self-similar fashion according to (2)-(4). The occupation numbers at small energies become larger and larger. At the certain moment t_0 , given by Eq. (7), close to the formal blow-up time t_* of the solution (2)-(4), the self-similarity of the energy distribution breaks down. The distribution gradually becomes bimodal, the low-energy quasi-condensate part of the field sets to the state of superfluid turbulence characterized by a tangle of the vortex lines. The further evolution of the quasi-condensate is independent of the rest of the system (apart from a permanent flux of the particles into the quasi-condensate) and basically is the process of relaxation of superfluid turbulence. All vortex lines relax in a macroscopically large time.

In conclusion, we note that our numerical approach can be extended to the case of a trapped Bose gas by simply including a term with an external potential in (1). Such a simulation could provide a deeper interpretation of the first experiment on the kinetics of BEC formation [16], as well as a precise understanding of the conditions and characteristic features of the full-scale scenario in the external potential [17].

NGB was supported by the NSF grants DMS-9803480 and DMS-0104288. BVS acknowledges a support from Russian Foundation for Basic Research under Grant 01-02-16508. The authors are very grateful to Professor Paul Roberts for fruitful discussions.

-
- [1] B.V. Svistunov, J. Moscow Phys. Soc. **1**, 373 (1991).
 - [2] Yu. Kagan, B.V. Svistunov, and G.V. Shlyapnikov, Zh. Eksp. Teor. Fiz. **101**, 528 (1992) [Sov. Phys. JETP **75**, 387 (1992)].
 - [3] Yu. Kagan and B.V. Svistunov, Zh. Eksp. Teor. Fiz. **105**, 353 (1994) [Sov. Phys. JETP **78**, 187 (1994)].
 - [4] M.H. Anderson *et al.*, Science **269**, 198 (1995); K.B. Davis *et al.*, Phys. Rev. Lett. **75**, 3969 (1995); C.C.

- Bradley *et al.*, Phys. Rev. Lett. **78**, 985 (1997).
- [5] A. Robert *et al.*, Science Express 10.1126/science.1060622 (2001); F. Pereira Dos Santos *et al.*, Phys. Rev. Lett. **86**, 3459 (2001).
- [6] V.L. Ginzburg and L.P. Pitaevskii, Zh. Eksp. Teor. Fiz. **34**, 1240 (1958) [Sov. Phys. JETP **7**, 858 (1958)]; E.P. Gross, Nuovo Cimento **20**, 454 (1961); L.P. Pitaevskii, Soviet Physics JETP, **13**, 451 (1961).
- [7] E. Levich and V. Yakhot, J. Phys. A: Math. Gen. **11**, 2237 (1978).
- [8] Yu. Kagan and B.V. Svistunov, Phys. Rev. Lett. **79**, 3331 (1997).
- [9] B.V. Svistunov, “*Kinetics of Strongly Non-Equilibrium Bose-Einstein Condensation*”, in Springer Lecture Notes in Physics series, 2001 (cond-mat/0009368).
- [10] K. Damle, S.N. Majumdar, and S. Sachdev, Phys. Rev. A **54**, 5037 (1996).
- [11] P.D. Drummond and J.F. Corney, Phys. Rev. A, **60**, R2661 (1999). The all-quantum simulation performed in this paper is similar to solving the GP equation.
- [12] D.V. Semikoz and I.I. Tkachev, Phys. Rev. D **55**, 489 (1997).
- [13] C. A. Jones and P. H. Roberts, J. Phys. A: Gen. Phys. **15**, 2599 (1982).
- [14] The weak-turbulence evolution is invariant to the details of the statistics of $|a_{\mathbf{k}}|$. By the time the system enters the regime of strong turbulence, the proper statistics is established automatically, since each harmonic participates in a large number of scattering events. We tried different distributions for $\xi_{\mathbf{k}}$ and saw no systematic difference in the evolution picture. The main set of our simulations was done with the distribution function $w(\xi_{\mathbf{k}}) = \exp(-\xi_{\mathbf{k}})$ (heuristically suggested by equilibrium Gibbs statistics of harmonics in the non-interacting model).
- [15] In the regime of weak turbulence, when there is no quasi-condensate, the procedure of filtering is ambiguous: the distribution is not bimodal, so there is no special low momentum k_c ; also, the structure of the defects in the filtered field essentially depends on the cut-off parameter, and thus has no physical meaning.
- [16] H.-J. Miesner *et al.* Science **279**, 1005 (1998).
- [17] B.V. Svistunov, cond-mat/0009295 (to be published in Phys. Lett. A).